ISBN: 978-3-95450-222-6 ISSN: 2673-5350 doi:10.18429/JACoW-IBIC2020-THPP16

SEPTUM ORBIT FEEDFORWARD CORRECTION AT THE AS

C. Lehmann*, University of Queensland, Brisbane, Australia
Y.-R. E. Tan, M. Atkinson, AS - ANSTO, Clayton, Australia

Abstract

The leakage fields generated by the septum in the injection straight perturbs the beam by as much as 130 µm horizontally and 80 µm vertically during injection. Passive shielding with copper collars and Mu metal sheets has reduced the perturbation but not removed them. The remainder of the perturbation will be corrected using an active feedforward system. This report will discuss the design of the system and the effectiveness of the prototype.

INTRODUCTION

The injection scheme in the storage ring is composed of four injection kicker magnets to create a local bump and two horizontal septa (SEP and SEI) to guide the electrons from the injector system into the storage ring. The arrangement of the septa is shown in Fig. 1 and ideally have no influence on the stored beam. As is commonly found, this is not the case due to stray fields and in 2016 we embarked on a project to improve the beam stability by reducing the effect of the two septa on the stored beam. This report will outline the steps taken, both passive and active measures to remove the disturbance.

Passive Shielding

To shield the stored beam from stray fields from SEI, 5 layers of 0.25 mm mu-metal are rolled around the vacuum chamber covering 1100 mm of the storage ring vacuum chamber. The mu-metal was rolled tight to maximise the inter-layer magnetic coupling with kapton tape wrapped around the vacuum chamber to insulate it from the mu-metal. A single layer of omega shaped mu-metal around 90% of the vacuum chamber circumference and loosely coupled to the septa shield plate was installed in one hard to reach section. SEI was run and inspected for arcs and unusual noises, none were found and the mu-metal foil did not appear to vibrate. Two copper boxes were then installed to shield the septa themselves as some parts of the vacuum chamber did not lend themselves to shielding, in particular near the septa ends which appear to have large fringing fields. The copper shield reduced the peak field measured 100 mm from the septa surface by an order of magnitude, it was not possible to measure the shielding effect of the mu metal. Figure 2 shows that these measures reduced the beam disturbance by only 44%. This result indicates that the majority of the disturbance is not due to the stray septum field hence not easily mitigated by shielding. Induced currents up to 30A were observed in the beam pipe and ground circuits, these may have contributed to the disturbance.

To use active compensation to remove the remaining disturbance would require a dipole kick of 10 µrad and 6.5 µrad in the horizontal and vertical planes, with a bandwidth of 2 kHz. This is outside the bandwidth of the Fast Orbit Feedback System [1] at 450 Hz. Therefore a separate feedforward system is required to compensate for this disturbance.

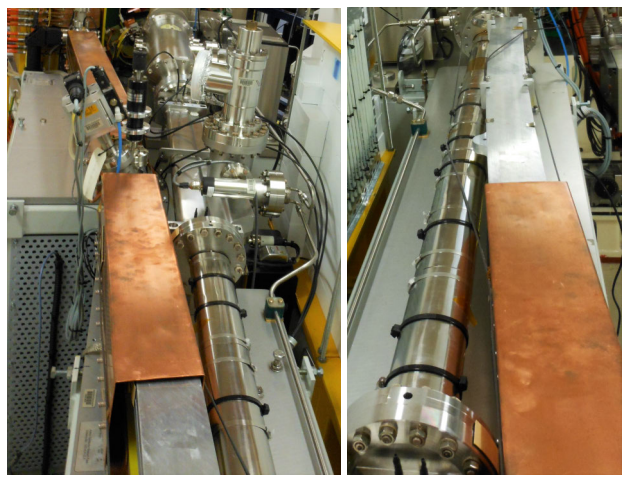

Figure 1: Location of SEP (top of left photo) and SEI (bottom of left photo). Passive shielding using copper sheets around the septa and mu metal sheets around the closest beam chambers (right photo).

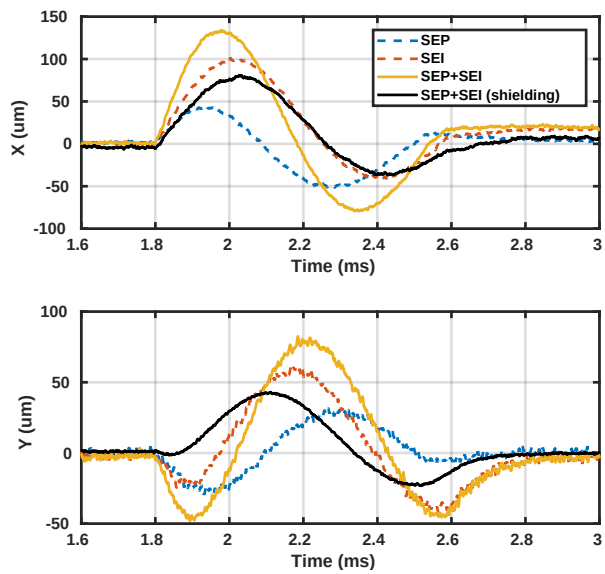

Figure 2: Perturbation from the two septa from turn-by-turn data (1.4 MS/s) and showing the effect of passive shielding that has been installed. Maximum amplitudes reduced from 134.1 µm and 80.5 µm to 80.2 µm and 42.7 µm.

* c.lehmann@uqconnect.edu.au

ISBN: 978-3-95450-222-6 ISSN: 2673-5350 doi:10.18429/JACoW-IBIC2020-THPP16

PERTURBATION MODELLING

The effects of the stray fields from the septum on the beam position throughout the storage ring can be modelled using closed orbit perturbation theory. When modelling the disturbance of a single dipole around the ring, it becomes useful to apply a Floquet transformation to change from the standard (s,x,y) closed orbit coordinates to (ψ, η_x, η_y), as outlined in Reference [2]. In these new coordinates a single dipole kick will cause a sinusoidal perturbation in (η, ψ) space, as described by

$$\eta = \eta_0 \cos(Q\psi + \lambda). \quad (1)$$

However, Eq. 1 is only valid in the domain $[\psi_k, 2\pi]$ where ψ_k is the phase position of the dipole kick. [2] does not correct for this. Once the domain is corrected to $[0, 2\pi]$, η_0 is substituted in, a phase offset λ is calculated to provide closed orbit continuity and the Floquet transform is reversed, the final expression used to describe a single dipole perturbation along an axis of the storage ring is given by,

$$x(s) = \left(\frac{\sqrt{\beta_x(s)\beta_{kx}}}{2|\sin \pi Q_x|} \frac{\delta(Bl)}{B\rho} \right) \cos(Q_x|\psi(s) - \psi_k| - (Q_x - \lfloor Q_x \rfloor)\pi) \quad (2)$$

where x(s) is the deviation along a closed orbit axis as a function of position, β_x is the beta function as a function of position, β_{kx} is the value of the beta function at the dipole location, Q_x is the tune, $\delta(Bl)$ is the dipole kick amplitude, $B\rho$ is the beam rigidity, $\psi(s)$ is the phase as a function of position and ψ_k is the phase at the dipole location.

By using the beta functions, tunes and phases taken from models of the storage ring, Eq. 2 can be used to predict the perturbation around the stored beam due to a dipole kick. The perturbation from the septa was found to be well modelled as a dipole kick, and fits the shape described by Eq. 2.

Dipole Location Modelling

Equation 2 was used to model the optimal location of the dipole corrector by using iterative methods to minimise and measure the net disturbance over the duration of the perturbation. It was also used to find the optimal current waveform for each correction dipole location.

By simulating the effectiveness of a range of locations around the storage ring in MATLAB, the optimal location was found to be immediately adjacent to the septum 2 meters upstream of the injection. Since it also proved convenient to access, this location was chosen for the prototype.

COIL OPTIMISATION

An initial prototype correction dipole was constructed, consisting of 4 pre-wound coils of 1.0 mm copper wire with approximately 200 turns of 30 mm diameter, mounted on the bellows with 1 coil on each side. The coils along each axis were connected in series and driven by a 50V/2A Kepco power supply in current mode. Initial testing of this prototype was partially successful in cancelling the perturbation. With this prototype, kicks of 1.2 µrad were achieved on both x and y axes using the maximum current of 2 A and approaching the 50 V capability of the power supply. This fell short of the 10 µrad and 6.5 µrad kick strengths required to fully cancel the perturbation on the x and y axes respectively. Since using larger power supplies was impractical the required kick amplitude had to be achieved by optimising the coil design and mounting arrangement.

There were two options for the mounting location: on the vacuum tube or bellows. The vacuum tube has a 2 mm thick stainless steel outer layer, and as such will cause significant attenuation and give a noticeable low-pass filter effect to any magnetic field waveform transmitted through it. The bellows have only very thin stainless steel layers and as such will not have significant frequency effects. However, the bellows mounting requires the coils to be mounted further from the beam reducing the effective field. These options will be compared to determine which produces the larger kick amplitude.

Geometry Optimisation

To optimise the coils and increase the kick amplitude, the constraints of the system were evaluated. The total kick strength from a single dipole can be modelled as the compound of the magnetic field produced by a solenoid and the length over which it effects the beam, given by the expression $Bl = \mu NIl/h$. Since the current is already maximised at 2 A, the value of Bl can be most easily increased by increasing the number of turns, increasing the length of the field, and decreasing the height of the magnet (increasing the coil density). For a power supply providing 2 A at 1 kHz with a voltage limit of 50 V, the maximum inductance per coil is calculated to be 2 mH. Since the inductance of a coil is given by the expression $L = \mu N^2 lw/h$, the kick strength can be increased within this inductance constraint by reducing the number of turns, increasing the length and reducing the coil thickness/height.

FEMM Analysis

To investigate these phenomenon further, Finite Element Method Magnetics (FEMM) was used to optimise the coil geometry and compare the two mounting options (bellows or directly on the vacuum chamber). The vacuum chamber cross-section was measured and placed in the simulation, while the bellows were modelled as air. The simulations showed the 1 kHz magnetic field at the beam produced by a vacuum chamber mounting is a factor of 2 better than a bellows mounting, despite the associated frequency effects. As such, to maximise the kick amplitude a vacuum tube mounting was the better option.

The results of this FEMM analysis were later experimentally verified using a frequency sweep with both bellows and vacuum tube mountings. At 1 kHz, the vacuum tube mounting showed a significantly higher kick amplitude.

ISBN: 978-3-95450-222-6 ISSN: 2673-5350 doi:10.18429/JACoW-IBIC2020-THPP16

SETUP

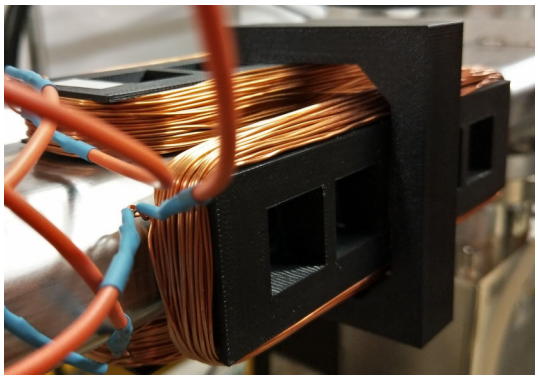

Figure 3: Final coil design with a 3D printed holder to clamp the coils around the vacuum chamber.

The final prototype seen in Fig. 3 consists primarily of a 3D printed mounting and 3 hand-wound air coils of dimension (150 × 40 × 15) mm. The top and bottom coils are connected in series, and each set of cables are fed out of the tunnel to two 50V/2A Kepco power supplies (horizontal and vertical corrector coils). Each power supply is set to Current mode, and provided a voltage waveform by a RedPitaya [3, 4]. The power supplies have been modified such that the +1 to -1 Volt signal from the RF Output channel of the RedPitaya produces a corresponding output current of +2 to -2 Amps from the power supply. Custom voltage waveforms are uploaded to the RedPitaya for each axis as retrieved from the perturbation modelling optimisation. The RedPitaya is triggered by the timing system [5] to generate one waveform synchronised to the storage ring injection. The EPICS interface was used to calibrate the prototype such that the amplitude and timing of its perturbation opposes the perturbation from the septum.

RESULTS

The implementation of active feedforward correction was successful in removing the perturbation from the septum. Figure 4 displays the perturbation cancellation across all BPMs at the moment of maximum perturbation for each axis. Figure 5 indicates this result remains consistent through the entire 1ms duration.

Figure 5 was created by taking the RMS closed orbit deviation across all BPMs for each time sample. The Passive+Active method shows the maximum RMS perturbation was able to be reduced further than by the Passive method alone, from 19.9 µm to 4.5 µm horizontally and from 14.1 to 3.4 µm vertically, a further reduction of over 75% on each axis.

The noise floor may be seen to vary from 1–2 µm. On the Y axis perturbations have been cancelled to the level of the noise floor, but the X axis still shows some minor perturbations. Figure 4 also shows some minor perturbation across some BPMs on the x axis. These remaining perturbations are likely caused by a number of factors. Some error is expected from the calibration process in both the trigger

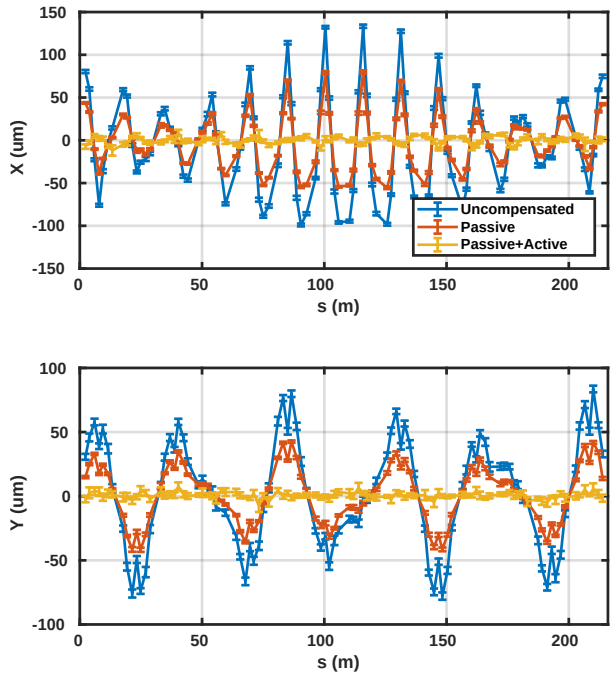

Figure 4: Maximum orbit perturbation at the 2 ms (X) and 2.2 ms (Y) before any compensation, with passive and with combined measures.

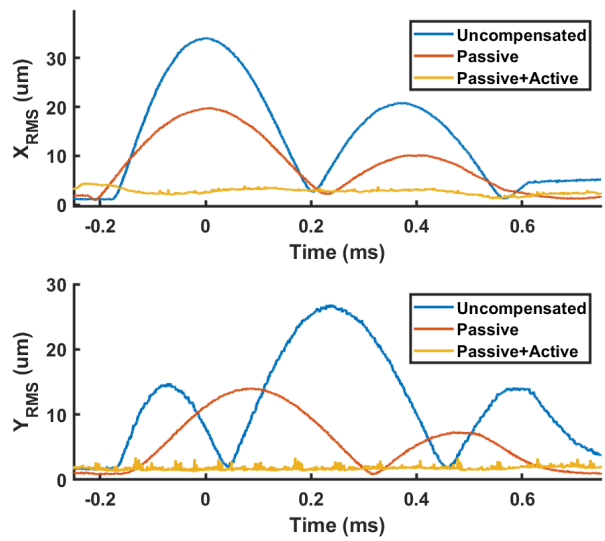

Figure 5: RMS orbit perturbation across all BPMs over full duration before any compensation, with passive and with combined measures.

timing, shape and amplitude of the compensation waveform, but this can be reduced in a later design through iterative optimisation. There is expected to be further error from the distortion of the dipole's magnetic field due to the frequency effects of the vacuum tube. Finally, the perturbation modelling optimisation indicated some minor perturbations would remain due to the co-positioning of the x and y axis correction dipoles, a sacrifice made for convenience.

ISBN: 978-3-95450-222-6 ISSN: 2673-5350 doi:10.18429/JACoW-IBIC2020-THPP16

CONCLUSION

The design and testing of an active feedforward perturbation compensation prototype demonstrates a method for reducing perturbations from the septum with far greater effectiveness than passive shielding alone. By adding active compensation, the net perturbation was able to be further reduced by 75% on each axis such that remaining perturbations approach the noise floor. A more permanent version of this prototype still remains to be constructed.

ACKNOWLEDGEMENTS

Would like to thank the help from Andraz Pozar from the Controls group to help with setting up the EPICS driver for the RedPitaya.

REFERENCES

[1] Y. E. Tan *et al.*, "Commissioning of the Fast Orbit Feedback System at the Australian Synchrotron", in *Proc. IPAC'17*, Copenhagen, Denmark, May 2017, pp. 1770–1773. doi:10.18429/JACoW-IPAC2017-TUPIK040

[2] E. J. N. Wilson, "Imperfections and multipoles", *An Introduction to Particle Accelerators*, Oxford, UK, Oxford University Press, 2001, pp. 77–79. doi:10.1093/acprof:oso/9780198508298.001.0001

[3] Red Pitaya, https://www.redpitaya.com/.

[4] Red Pitaya - EPICS driver (Australian Synchrotron), https://github.com/AustralianSynchrotron/redpitaya-epics

[5] E. D. van Garderen, G. LeBlanc, A. C. Starritt, K. Zingre, and M. L. M. ten Have, "Upgrade of the Timing System at the Australian Synchrotron", in *Proc. DIPAC'09*, Basel, Switzerland, May 2009, paper TUPD27, pp. 357–359.